NJC

PAPER

View Article Online
View Journal

Cite this: DOI: 10.1039/c8nj02628a

The influence of oxidative debris on the fragmentation and laser desorption/ionization process of graphene oxide derivatives†

Yu Lim Hong,[ab] Jieon Lee,[c] Bon-Cheol Ku,[a] Kyungtae Kang,[d] Seunghyun Lee,[e] Seongwoo Ryu[b] and Young-Kwan Kim *[a]

Received 28th May 2018,
Accepted 22nd June 2018

DOI: 10.1039/c8nj02628a

rsc.li/njc

The effect of oxidative debris (OD) on the fragmentation behavior and the laser desorption/ionization (LDI) process of graphene oxide (GO) derivatives was systematically investigated to explore the potential of LDI time-of-flight mass spectrometry (LDI-TOF-MS) as a characterization tool for their chemical structure and photochemical properties. Based on the results, we found that the fragmentation patterns and the LDI properties of the GO derivatives were highly affected by the OD adsorbed on their surface. Our findings suggest that LDI-TOF-MS can be a useful analytical tool for determining the chemical structure and photochemical properties of GO derivatives.

Introduction

Graphene oxide (GO) has been investigated extensively owing to its unique physicochemical properties for various applications including catalysts, nanocomposites, biosensors and theranostics.[1] The origin of its unique properties was initially attributed to its traditional single-component model, which suggested that GO is composed of a single layered sp^2 carbon sheet mainly decorated with hydroxyl- and epoxy groups on its basal plane and with carboxylic acids on its edge.[2] However, Rourke *et al.* suggested a two-component model, where GO consists of a graphene-like sheet and surface adsorbed oxidative debris (OD), by showing that it can be separated by a base-washing process.[3] Accordingly, the origin of electrochemical activity,[4] adsorptivity,[5] and fluorescence[6] of GO was attributed to the OD layer rather than the graphene-like sheet itself.

In contrast, Dimiev *et al.* refuted the two-component model based on their observation that GO was cleaved by a hydroxide ion during base washing. They claimed that the material released during the washing was not OD, but rather a fragment of GO generated by the nucleophilic attacks of the hydroxide ions.[7] Chen *et al.*, however, directly observed OD on GO by using high resolution transmission electron microscopy (HR-TEM),[8] and Rourke *et al.* reported a letter that rationally defended the two-component model of GO.[9] Although the debate on the real structure of GO is ongoing, the existence of OD on GO is experimentally confirmed by those efforts.

Recently, Eigler *et al.* investigated the fluorescence properties of GO by using various mixtures of OD and less defective GO, and demonstrated that the optical properties of GO originated from its oxygenated hexagonal sp^2 carbon framework rather than OD.[10] This study suggests a contradictory conclusion to the previous report, which reported that the fluorescence of GO is mostly derived from the surface adsorbed OD.[6] This inconsistency implied that the real role of OD in various photochemical processes is still unclear and it motivates a further systematic approach.

In this regard, laser desorption/ionization time of flight mass spectrometry (LDI-TOF-MS) analysis on GO derivatives is an interesting photochemical process wherein GO derivatives convert laser energy into thermal energy, and then enable the LDI-TOF-MS analysis of small molecules.[11] We have reported that the efficiency of LDI-TOF-MS analysis on GO derivatives varies depending on their lateral dimensions and photothermal properties because small GO has more stable chemical structures and higher photothermal conversion efficiency than large GO.[12] Based on our previous results, we hypothesized that there might be a veiled role of OD in the LDI-TOF-MS process of GO derivatives. In addition, LDI-TOF-MS analysis can be directly used as an analytical tool to investigate the chemical structures and photochemical properties of GO derivatives as graphite-like

[a] Carbon Composite Materials Research Center, Institute of Advanced Composite Materials, Korea Institute of Science and Technology, San 101, Eunha-ri, Bongdong-eup, Wanju-gun, Jeollabuk-do, 565-905, Korea. E-mail: youngkwan@kist.re.kr
[b] Department of Advanced Materials Engineering, University of Suwon, Hwaseong-Si, Gyeonggi-do, 445-743, Korea
[c] Predictive Toxicology Department, Korea Institute of Toxicology, 141 Gajeong-ro, Yuseong-gu, Daejeon, 34114, Korea
[d] Department of Applied Chemistry, Kyung Hee University, Yongin, Gyeonggi-do 446-701, South Korea
[e] Department of Nanochemistry, Gachon University, Sungnam, Gyeonggi 13120, Republic of Korea

† Electronic supplementary information (ESI) available: The additional experimental procedure and results. See DOI: 10.1039/c8nj02628a

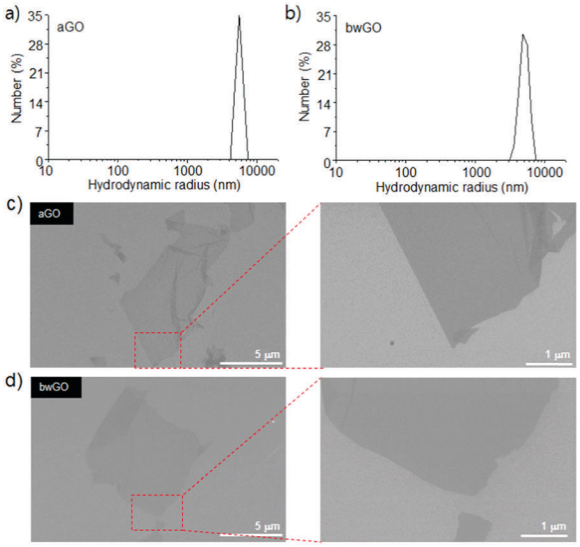

Fig. 1 (a) Hydrodynamic radii of aGO and (b) bwGO. (c) SEM images of aGO and (d) bwGO at different magnifications showing their edge structures.

materials are fragmented into carbon cluster ions with characteristic patterns under high power laser irradiation, which induces a rapid heating process.[13,14]

Herein, we carried out base-washing of the as prepared GO (aGO) to dissociate OD from a graphene-like sheet, which is termed base-washed GO (bwGO) (Fig. 1a).[15] We first analysed these GO derivatives with conventional characterization tools for systematically comparing them with those evaluated by our LDI-TOF-MS analysis to reveal the influence of OD on the fragmentation and photothermal conversion properties of the GO derivatives (Fig. 1b). Based on the LDI-TOF-MS analysis results, we concluded that the fragmented cluster ions from aGO mainly originate from OD (inferred from its fragmentation behaviour) and it significantly affects the efficiency of the GO derivatives as a matrix for LDI-TOF-MS analysis.

Experimental

Materials

Natural graphite (FP 99.95% pure) was purchased from Graphit Kropfmühl AG (Hauzenberg, Germany). Potassium permanganate, sodium nitrate, sodium hydroxide, ethanol, hydrochloric acid, sulfuric acid and hydrogen peroxide (30% in water) were purchased from Daejung Chemicals (Siheung, Korea). Ascorbic acid, glucosamine, sucrose and glucose were purchased from Alfa Aesar (Ward Hill, MA). All chemicals were used as received.

Preparation of aGO

1.5 g of graphite powder and 0.5 g of sodium nitrate were added in 23 mL of sulfuric acid and stirred for 5 min. 3 g of potassium permanganate was slowly added to the acid mixture with stirring in an ice bath. After addition, the mixture was transferred to a water bath at 35 °C and stirred for 1 h. 40 mL of water was gradually added to the mixture, stirred for 30 min and diluted with 100 mL of water in an ice bath to avoid a rapid increase of the temperature because this step is highly exothermic. Finally, 3 mL of hydrogen peroxide (30%) was added dropwise to the mixture with color change to bright yellow. The reaction mixture of graphite oxide was centrifuged at 10 000 rcf and washed with 3.5% hydrochloric acid three times to remove metal salts. Then, the graphite oxide was neutralized by repeated centrifugation and washing with a copious amount of water. After neutralization, the aGO suspension was obtained at 1 mg mL^{-1}.

Preparation of OD and bwGO from aGO

140 mg of sodium hydroxide was added to 250 mL of the aGO suspension (0.5 mg mL^{-1}) with stirring and heated to 70 °C for 1 h. After centrifugation of the reaction mixture at 15 870 rcf, the supernatant was collected, neutralized with 1 M HCl. The precipitates were also neutralized with 1 M HCl and then further purified by repeated centrifugation and washing with water to obtain bwGO.

Synthesis of benzylpyridinium salt (BP)

7.8 g of benzyl bromide (45.5 mmol, 5.4 mL) was added to 3.0 g of pyridine (37.9 mmol, 3.05 mL) in a 20 mL scintillation vial with stirring. The reaction was carried out at 50 °C overnight. Afterwards, the formed precipitate was washed with diethyl ether, filtered, and washed with a copious amount of diethyl ether to form the BP (95% yield).

LDI-TOF-MS analysis

1 μL of OD, bwGO and aGO suspensions (1 mg mL^{-1}) was respectively deposited on a stainless steel plate, dried under ambient conditions and subjected to LDI-TOF-MS analysis. All mass spectrometric analyses were carried out by using a Bruker Autoflex III instrument (Bruker Daltonics, Germany) equipped with a Smartbeam laser (Nd:YAG, 355 nm, 100 Hz, 100 μJ in laser power, 50 μm in spot diameter at target plate) in the negative reflective mode for OD, bwGO and aGO (80% laser power), and in the positive reflection mode for small molecules (40% laser power). The ionization mode was selected on the basis of the preferential ionization behaviour of the analytes. The accelerating voltage was 19 kV and all spectra were obtained by averaging 500 laser shots unless otherwise indicated.

Characterization

The hydrodynamic radii of aGO and bwGO were determined by using a Nano ZS instrument (Malvern, UK). Their lateral sizes and edge structures were observed by using a NOVA NanoSEM 450 instrument (FEI company, Netherlands). Single-layer exfoliation of the GO derivatives was confirmed by using atomic force microscopy (AFM) (XE-100, Park System, Korea) with a backside gold-coated silicon SPM probe (Park System, Korea). UV-Vis spectra were obtained using a J670 instrument (Jasco, Japan). Fourier transform infrared (FT-IR) analysis was performed by using a Nicolet iN10 microscope (Thermo Scientific, USA) in a reflective mode. Raman spectra were obtained by using a HORIBA LabRAM instrument (Jobin Yvon, France) using an air-cooled He/Ne laser (514 nm) as an excitation source focused

through an integral microscope (Olympus BX 41). Thermogravimetric analysis (TGA) was carried out by using a TGA Q 50 instrument (TA instruments, USA). Raman signal was recorded with 180° geometry using an air-cooled 1024 × 256 pixel CCD detector. The X-ray diffraction (XRD) patterns of aGO and bwGO were obtained using a X-ray diffractometer (D/MAX 2500, Rigaku) with Cu Kα radiation (λ = 0.15418 nm) at 40 kV and 50 mA. The scan rate was 2° min^{-1} for 2θ values between 5 and 60°. X-ray photoelectron spectroscopy (XPS) analysis was performed using a Thermo Scientific K-alpha instrument (Thermo VG, USA) using monochromated Al Kα radiation (1486.6 eV).

Results and discussion

aGO was synthesized by the previously reported method,[12] washed with 0.01 M NaOH at 70 °C for 1 h to release OD from aGO, and centrifuged at 15 870 rcf for 1 h to separate OD from bwGO.[15] A high centrifugal force is required to collect the possible fragmented pieces of aGO and compare the size distribution of bwGO with that of aGO. Then, OD and bwGO were neutralized with 1 M HCl to exchange the sodium cations with protons. bwGO was further purified by repeated centrifugation and washing with water. The sheet sizes of aGO and bwGO were analysed by dynamic light scattering (DLS) and SEM. Their size distributions were similar to each other (Fig. 1a, b and Fig. S1 in the ESI†) and no jagged edge on bwGO was observed (Fig. 1c, d and Fig. S2, ESI†). In the case of OD, direct imaging with electron microscopy is quite challenging because it is too small and labile to be damaged by the E-beam.[9] The single layer exfoliation of aGO and bwGO was confirmed by AFM analysis (Fig. S3, ESI†). These results suggested that there was no significant fragmentation of aGO and re-stacking of the exfoliated aGO during the base-washing process.

aGO, OD, and bwGO were analysed by using UV-Vis spectroscopy. The UV-Vis spectrum of aGO showed a typical peak at 233 nm due to the π–π* transition of the aromatic C═C bonds and a shoulder at around 300 nm due to the n–π* transition of the C═O bonds (Fig. 2a).[16] OD did not show clear π–π* and n–π* transition peaks (Fig. 2a). This distinct optical feature of OD was predictable, because of its highly oxidized structure.[3] bwGO exhibited a π–π* transition peak at the equal position to that of aGO after the base washing process (the detachment of OD), but there was an increase in the absorption in the visible region (Fig. 2a). These results suggest that the base washing process resulted in only a slight and partial reduction of aGO and thus there was no extension of the existing conjugated structures in aGO (Fig. 2a).

TGA analysis was performed under a nitrogen atmosphere to estimate the proportion of OD in aGO. The TGA curves of aGO and bwGO showed typical weight loss points at around 100 and 200 °C, which originated from the evaporation of the adsorbed water and the decomposition of OD.[3] The TGA curve of aGO exhibited 5.24% weight loss at 100 °C and the weight loss reached 39.69% at 200 °C (Fig. 2b). bwGO also presented a similar weight loss tendency at 100 °C (4.02%) and 200 °C (30.65%) (Fig. 2b). After the separation of OD, the weight loss at 200 °C was still observed in bwGO, which might be attributed to the decomposition of the oxygen containing functional groups on its carbon framework. This result indicated that the amount of intercalated water in aGO and bwGO was analogous and the proportion of OD in aGO was around 9.04%.

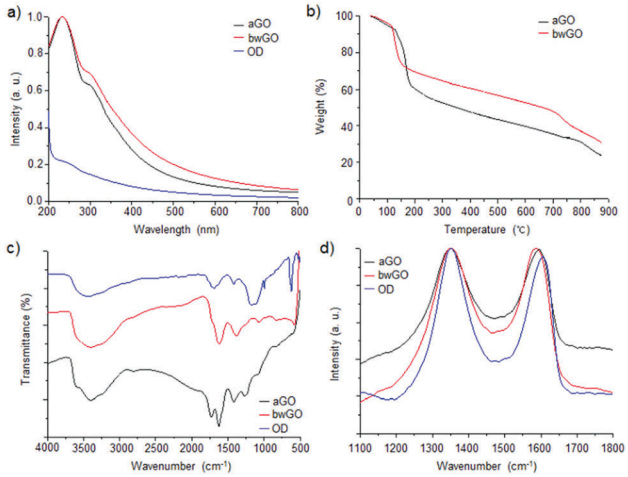

Fig. 2 (a) UV-Vis, (b) TGA, (c) FT-IR, and (d) Raman spectra of aGO, bwGO, and OD.

The FT-IR spectrum of aGO showed characteristic peaks at 1068 cm^{-1} (the C–OH stretching of the hydroxyl group), 1265 cm^{-1} (the C–O–C vibration of the epoxy group), 1411 cm^{-1} (the O–H bending of the hydroxyl group), 1623 cm^{-1} (the bending mode of the intercalated water), 1731 cm^{-1} (the C═O stretching of the carboxylic acid group), and 3386 cm^{-1} (the O–H vibration of the hydroxyl group) (Fig. 2c).[17] After base-washing, although the peaks derived from the hydroxyl groups of the GO derivatives were negligibly changed, bwGO presented the disappearance of the C–O–C vibration peak, a weakened C═O stretching peak at around 1716 cm^{-1}, a broad peak at 1619 cm^{-1} and a symmetric stretching peak of the carboxylate ion at 1380 cm^{-1} (Fig. 2c). The absence of C–O–C vibration indicated that most of the epoxy groups of aGO were diminished upon base washing. The broad peak at 1619 cm^{-1} was attributed to the stretching of the carboxylate ions.[7] The C–O–C vibration was not observed for OD, but the stretching mode of the carboxylate ion was more strongly observed for OD with the appearance of new peaks at around 1122 cm^{-1} originated from one carbon atom vacancy in its surface (Fig. 2c).[18] These results proved that OD has a more carboxylated and damaged structure compared to aGO and bwGO, and suggested that the base-washing step led to the removal of the epoxy groups and the deprotonation of the carboxylic acid groups on OD and bwGO, which facilitated their dissociation by electrostatic repulsion.

The characteristic D and G peaks of aGO, bwGO and OD were observed in their Raman spectra (Fig. 2d)[8,19] and their relative D and G peak intensity ratios (D/G ratio) were 1.01, 1.00 and 1.04, respectively. These indicated that the sp^2 carbon structure was relatively preserved in bwGO compared to aGO and OD. Although several previous reports suggested that OD

did not show D and G peaks owing to no extended sp^2 carbon domain,[3,20] D and G peaks were observed for the present OD with a high D/G ratio (1.04) compared to those of aGO (1.01) and bwGO (1.00), which were also observed for OD prepared by a similar process (Fig. 2d).[8] This discrepancy might result from the different synthetic conditions of aGO such as starting natural graphite, oxidation time, and exfoliation and purification processes. Taking the results from spectroscopic analyses together, we could confirm that OD was separated from aGO and contained highly oxidized and damaged sp^2 carbon structures compared to aGO and bwGO.

aGO, bwGO and OD were then analysed by LDI-TOF-MS to investigate their fragmentation behaviour. The negative ionization mode was chosen because the positive ionization mode led to the formation of undesired cation adducts from the residual Na^+ and K^+ ions on the surface of aGO, which hampered the interpretation of the mass spectra (Fig. S4, ESI†).[3,10,21] GO derivatives undergo photothermal fragmentation during LDI-TOF-MS analysis under high power laser irradiation.[22] aGO showed fragmented carbon clusters at m/z 24 $[C_2]^-$, 36 $[C_3]^-$, 48 $[C_4]^-$, 60 $[C_5]^-$, 72 $[C_6]^-$, 84 $[C_7]^-$, 96 $[C_8]^-$, 108 $[C_9]^-$, and 132 $[C_{11}]^-$ and oxidized carbon clusters at m/z 44 $[C_1O_2]^-$, 80 $[C_4O_2]^-$, 96 $[C_4O_3]^-$, 120 $[C_6O_3]^-$, and 140 $[C_9O_2]^-$ (Fig. 3a).

The observed oxidized carbon clusters for aGO could have stemmed from the fragmentation of OD, which has a damaged and highly oxidized structure, or the direct fragmentation of aGO. If the oxidized carbon clusters have originated from OD, bwGO should exhibit less oxidized carbon clusters than aGO. As expected, when bwGO was analysed by using LDI-TOF-MS, carbon cluster ions were detected strongly at m/z 60 $[C_5]^-$, 72 $[C_6]^-$, 84 $[C_7]^-$, 96 $[C_8]^-$, 108 $[C_9]^-$, 120 $[C_{10}]^-$, 132 $[C_{11}]^-$, and 144 $[C_{12}]^-$, whereas the oxidized carbon cluster peaks weakened (Fig. 3b). This fragmentation behaviour implied that OD clearly exists on aGO and the oxidized carbon clusters might mainly originate from the fragmentation of OD rather than that of the graphene-like sheet. In addition, the strong signals of the carbon clusters from bwGO implied that bwGO has higher laser absorption and photothermal conversion efficiencies than aGO. This result concurred well with the stronger optical absorption of bwGO than that of aGO (Fig. 2a).

Interestingly, OD exhibited greatly higher carbon cluster peaks at m/z 60 $[C_5]^-$, 72 $[C_6]^-$, 84 $[C_7]^-$, 96 $[C_8]^-$, 108 $[C_9]^-$ and 120 $[C_{10}]^-$ than the oxidized carbon cluster peaks, much alike bwGO (Fig. 3c). The size and simulated m/z of OD were around 2.2 nm and in the range of 2400–2600 Da,[8] respectively, which suggested that the detected cluster peaks originated from the fragments of OD. Such similar fragmentation patterns of OD and bwGO (and the absence of the oxidized carbon cluster peaks therein) indicated that the oxygen containing functional groups of aGO were partially removed during the base washing process. The array of intense carbon cluster peaks in the mass spectra of bwGO and OD with a repeating unit of 12 Da clearly confirmed that the observed mass signals were derived from the graphite-like carbon structures.[23] These suggested that the base washing of aGO produces OD and bwGO, but also alters their chemical structures compared to those in their initial state. This also tells us that the chemically prepared OD does not represent the real OD, and thus cannot be used as a model to investigate the effect of pure OD on the physicochemical properties of aGO.

For further investigation of the influence of base-washing on the chemical structures of the GO derivatives, the XRD patterns of aGO, bwGO and OD were analysed and the interlayer distance of aGO and bwGO was specified by d-spacing of the (001) plane, d_{001}. The d_{001} values of aGO and bwGO were 7.34 Å and 7.18 Å, respectively (Fig. 4a). The smaller d-spacing of bwGO than that of aGO indicated the successful removal of OD from aGO. In the case of OD, there was only a strong signal from NaCl rather than a typical XRD pattern of the graphitic carbon materials owing to its highly oxidized structure and

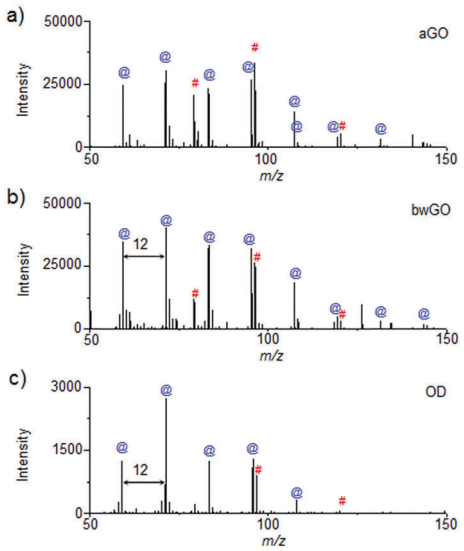

Fig. 3 (a) Mass spectra of aGO, (b) bwGO, and (c) OD obtained by LDI-TOF-MS analysis in the negative ionization mode. The symbol @ in blue corresponds to the carbon cluster ions while the symbol # in red corresponds to the oxidized carbon cluster ions.

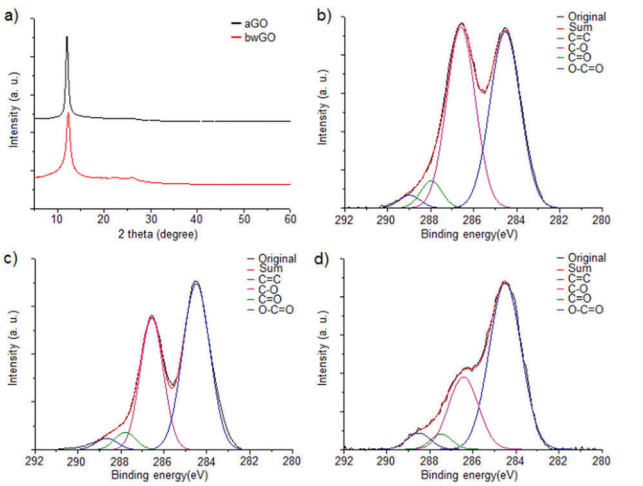

Fig. 4 (a) XRD patterns of aGO and bwGO. C 1s XPS spectra of aGO (b), bwGO (c), and OD (d).

small size,[3,20] and a possible interference from the NaCl crystals (Fig. S5, ESI†). Then, the GO derivatives were characterized by using XPS. The C 1s XPS spectrum of aGO showed typical peaks of the aromatic C═C, C–O, C═O and O–C═O bonds at 284.5, 286.2, 287.8, and 289.0 eV, respectively (Fig. 4b).[3] The C–O bond in the C 1s XPS spectrum of bwGO was relatively weakened (Fig. 4c). This transition matches well with the FT-IR characterization result and thus was attributed to both the release of OD and the removal of the epoxy groups (Fig. 2c). OD presented a more weakened C–O bond but slightly higher C═O and O–C═O bonds than bwGO, which indicated that the release of OD was accompanied with the loss of the C–O bonds from the epoxy groups of aGO (Fig. 4d and Fig. 2c). This result implied that the oxidized carbon clusters from the GO derivatives mostly originated from the cleavage of their oxidized carbon framework decorated with the epoxy groups during LDI-TOF-MS analysis (Fig. 3). The XPS analysis result was consistent with the FT-IR and LDI-TOF-MS analysis results and thus supported that this is a reliable characterization approach for GO derivatives.

Finally, the LDI-TOF-MS process of aGO, bwGO, and OD was investigated by using the benzylpyridinium salt (BP) as a thermometer molecule to determine the desorption efficiency (DE) and survival yield (SY) during LDI-TOF-MS analysis (Fig. 5a and b).[24,25] The DE and SY were determined by summing the intensity of the parent and fragment ions and dividing the parent ion intensity with the total intensity of the parent and fragment ions, respectively (Fig. 5b).[24,25] DE and SY are important parameters for LDI-TOF-MS analysis because these terms are directly related to the LDI efficiency and soft ionization potential of nanomaterials.[24,25] Especially, the SY is directly related to the extent of internal energy transferred from materials: a higher SY indicates a lower internal energy transfer.[24] The average values of DE for aGO was measured to be 12 446 and this value significantly increased to 38 531 for bwGO (Fig. 5c). Considering the low DE value of OD (1454) (Fig. 5c), it was found that OD interfered the LDI process on aGO. The average SY value of aGO was 45.3% and this value also increased to 62.1% for bwGO (Fig. 5c). This change implied that the presence of OD increased the internal energy required for the LDI of BP (Fig. 5c). These LDI studies of BP suggested that the LDI process of aGO predominantly occurs on the graphene-like sheet (bwGO) and it was interfered by the presence of OD, which might hinder the energy transfer from the graphene-like sheet to the analytes (see Fig. S6, ESI† for the LDI-TOF-MS analysis of various small molecules with aGO and bwGO). This is consistent with the previous results of Eigler *et al.*,[10] who demonstrated that the photochemical properties of aGO originated from a graphene-like sheet and not OD. Therefore, bwGO provided the higher photothermal conversion and energy transfer efficiencies for the LDI of the BP molecules than aGO.

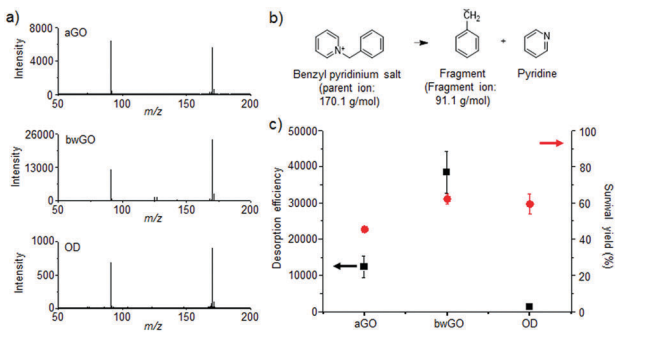

Fig. 5 (a) Mass spectra of BP obtained with aGO, bwGO, and OD. (b) Fragmentation process of BP during LDI-TOF-MS analysis. (c) The DE and SY of aGO, bwGO, and OD estimated in the equal positive ionization mode.

Conclusions

In conclusion, the fragmentation behaviour and photothermal conversion efficiency of aGO, bwGO and OD were systematically investigated by using LDI-TOF-MS, for the first time, and their structural implications and LDI properties were illuminated. LDI-TOF-MS analyses reveal that the oxidized carbon clusters from aGO primarily originated from the fragmentation of OD on its surface rather than its core carbon frameworks (bwGO). We also found that the oxidized carbon clusters of the GO derivatives were mainly produced from the fragmentation of the carbon frameworks decorated with epoxy groups, and the adsorbed OD on aGO adversely affected their LDI efficiency. Moreover, it was also revealed that the base-washing process of aGO resulted in not only the separation of OD from bwGO but also their chemical reduction, and thus the chemical structures of the separated OD and bwGO are different from their pristine counterparts in aGO. In this regard, the physicochemical properties of the chemically separated OD do not fully represent those of pure OD on aGO. Our results also demonstrated clearly that LDI-TOF-MS analysis is a useful and efficient tool—that enables the detection of what could not be seen using conventional tools—to analyse the chemical structure and photochemical properties of GO derivatives. Therefore, we conclude that this study offers an important and practical platform technique to investigate the structure and photochemical property relationship of nanomaterials.

Conflicts of interest

There are no conflicts to declare.

Acknowledgements

This research was financially supported by grants from the Korea Institute of Science and Technology (KIST) Open Research Program (ORP), the Nano·Material Technology Development Program through the National Research Foundation of Korea (NRF) funded by the Ministry of Science, ICT and Future Planning (2016M3A7B4027223), (2016M3A7B4905609) and (2016R1D1A1-B03932999), and the KIAT (Korea Institute for Advancement of Technology) grant (N0000992) funded by the Ministry of Trade, Industry and Energy, Republic of Korea.

Notes and references

1 Y. Zhu, S. Murali, W. Cai, X. Li, J. W. Suk, J. R. Potts and R. S. Ruoff, *Adv. Mater.*, 2010, **22**, 3906.
2 K. P. Loh, Q. Bao, G. Eda and M. Chhowalla, *Nat. Chem.*, 2010, **2**, 1015.
3 J. P. Rourke, P. A. Pandey, J. J. Moore, M. Bates, I. A. Kinloch, R. J. Young and N. R. Wilson, *Angew. Chem., Int. Ed.*, 2011, **50**, 3173.
4 A. Bonnani, A. Ambrosi, C. K. Chua and M. Pumera, *ACS Nano*, 2014, **8**, 4197.
5 D. Ma, L. Dong, M. Zhou and L. Zhu, *Analyst*, 2016, **141**, 2761.
6 H. R. Thomas, C. Valles, R. J. Young, I. A. Kinloch, N. R. Wilson and J. P. Rourke, *J. Mater. Chem. C*, 2013, **1**, 338.
7 A. M. Dimiev and T. A. Polson, *Carbon*, 2015, **93**, 544.
8 X. Chen and B. Chen, *Environ. Sci. Technol.*, 2016, **50**, 8568.
9 J. P. Rourke and N. R. Wilson, *Carbon*, 2016, **96**, 339.
10 A. Naumov, F. Grote, M. Overgaard, A. Roth, C. E. Halbig, K. Nørgaard, D. M. Guldi and S. Eigler, *J. Am. Chem. Soc.*, 2016, **138**, 11445.
11 J. Lee, J. Kim, S. Kim and D.-H. Min, *Adv. Drug Delivery Rev.*, 2016, **105**, 275.
12 Y.-K. Kim and D.-H. Min, *Chem. – Eur. J.*, 2015, **21**, 7217.
13 H. Kawasaki, N. Takahashi, H. Fujimori, K. Okumura, T. Watanabe, C. Matsumura, S. Takemine, T. Nakano and R. Arakawa, *Rapid Commun. Mass Spectrom.*, 2009, **23**, 3323.
14 K. Yoshimura, L. Przybilla, S. Ito, J. D. Brand, M. Wehmeir, H. J. Räder and K. Müllen, *Macromol. Chem. Phys.*, 2001, **202**, 215.
15 H. R. Thomas, S. P. Day, W. E. Woodruff, C. Vallés, R. J. Young, I. A. Kinloch, G. W. Morley, J. V. Hanna, N. R. Wilson and J. P. Rourke, *Chem. Mater.*, 2013, **25**, 3580.
16 Y.-K. Kim, M. H. Kim and D.-H. Min, *Chem. Commun.*, 2011, **47**, 3195.
17 C. Zhang, D. M. Dabbs, L. M. Liu, I. A. Aksay, R. Car and A. Selloni, *J. Phys. Chem. C*, 2015, **119**, 18167.
18 M. Acik, G. Lee, C. Mattevi, A. Pirkle, R. M. Wallace, M. Chhowalla, K. Cho and Y. Chabal, *J. Phys. Chem. C*, 2011, **115**, 19761.
19 C. Cong, T. Yu, K. Sato, J. Shang, R. Saito, G. F. Dresselhaus and M. S. Dresselhaus, *ACS Nano*, 2011, **5**, 8760.
20 Z. Guo, S. Wang, G. Wang, Z. Niu, J. Yang and W. Wu, *Carbon*, 2014, **76**, 203.
21 Y.-K. Kim, H.-K. Na, S.-J. Kwack, S.-R. Ryoo, Y. Lee, S. Hong, S. Hong, Y. Jeong and D.-H. Min, *ACS Nano*, 2011, **5**, 4550.
22 Y.-K. Kim and D.-H. Min, *ACS Appl. Mater. Interfaces*, 2012, **4**, 2088.
23 J.-S. Lee, Y.-K. Kim, J. Y. Hwang, H.-I. Joh, C. R. Park and S. Lee, *Carbon*, 2017, **121**, 479.
24 H. W. Tang, K. M. Ng, W. Lu and C. M. Che, *Anal. Chem.*, 2009, **81**, 4720.
25 Y.-K. Kim and D.-H. Min, *Langmuir*, 2014, **30**, 12675.

